ICAST2014 #068

Evaluation of the sensitivity and fatigue performance of embedded piezopolymer sensor systems in sandwich composite laminates

N A Chrysochoidis[1] and E Gutiérrez [1]

[1] European Commission, Joint Research Centre (JRC), Institute for the Protection and Security of the Citizen (IPSC), European Laboratory of Structural Assessment, Via Enrico Fermi 2749, 21027 Ispra VA, Italy, nikolaos.chrysochoidis@jrc.ec.europa.eu

Abstract

It has been claimed that embedding piezo-ceramic devices as structural diagnostic systems in advanced composite structures may introduce mechanical impedance miss-matches that favour the formation of intralaminar defects; this and other factors such as cost and their high strain sensitivity has motivated the use of thin-film piezo-polymer sensors. In this paper, we examine the performance of sandwich composite panels fitted with embedded piezopolymer sensors. Our experimental campaign examines both how such thin-film sensors perform within a structure and the converse effect; how the inclusion of sensor films affects structural performance. Strain-controlled tests on sandwich panels subjected to three-point bending under wide-ranging static and dynamic strains lead us to conclude that embedding thin piezopolymer films has no marked reduction on the tensile strength for a wide range of strain loading paths and magnitudes, and that the resilience of the embedded sensor is itself satisfactory, even up to the point of structural failure. Comparing base-line data obtained from standard surface-mounted sensors and foil gauges, we note that whereas it is possible to match experimental and theoretical strain sensitivities, key properties, especially the pronounced orthotropic electromechanical factor of such films must be duly considered before an effective calibration can take place.

1. INTRODUCTION

Advanced Composites are increasingly being used in an ever wider range of structural applications, and often promoted as one of the preferred host materials for sensor diagnostic systems. Composite materials' apparent amenity to host all manner of sensors promotes them as key candidates for, so called, smart structures; however, we are still far from fully understanding the effect of the sensor on the host's structural performance and, conversely, the effect of structure on the sensor's metrological capacity.

An embedded device in a composite structure generates a discontinuity that may affect the structural integrity. Thus, the placement of the sensor can be considered as an inclusion that not only results in the net area loss of the material, but may generate additional interlaminar stresses at, or near, the discontinuity within the host composite structure; this may result in a reduction of the load-carrying capability

The selection and integration of diagnostic and actuation devices within structural composites is as varied as their applications, including, amongst others: piezo-ceramics and piezo-polymers, fiber optics, shape memory alloys, strain sensors, and, more recently, the potential of creating a smart matrix system

based on the usage of nanoparticles. Lead Zirconate Titanate (PZT) has attracted the greatest attention with a wide range of sensor forms and materials: Crawley and De Luis, 1987; Warkentin and Crawley, 1991; Chow and Graves, 1992; Bronowicki, et al., 1996; Shukla and Vizzini, 1996; Mall and Coleman, 1998; Hansen and Vizzini, 2000; Yocum, et al., 2003 and Tang 'RAY', et al., 2011.

In our study we focus only on the use of polymer piezoelectric devices with a view to understanding the dual sensor—structure performance and functionality when exposed to high strains in both static and fatigue loading. In particular, we are interested in how the process of embedding larger Polyvinylidine Fluoride piezo-polymer films (PVDF) within the composite affects the laminate performance, and conversely, how the sensor is affected by being embedded in the structure and how it copes with sustained high strain excursions.

Another aspect of our study concerns more specific metrological aspects such as the theoretical versus experimental piezo-polymer strain sensitivity, material orthogonality and the potential of piezo-polymers to be used as low cost, low maintenance, multi-functional measurement and diagnostic systems.

PVDF is manufactured in, so-called, single and biaxial piezo-electric forms; i.e. isotropic and orthotropic. A calibration process must therefore consider whether, depending on the compliance properties of the host composite material, the type of PVDF used will significantly affect the calibration factors (Sirohi and Chopra, 2000). As we shall show, when PVDF sensors are incorporated into highly-anisotropic composite lay-ups the effect of the host material's Poisson ratio or the orientation of the piezo-film in the predominate principal stress plane may couple the orthotropic piezo-properties with unexpected results.

The potential of using piezoelectric polymer films as monitoring devices in composites follows soon after their discovery in the late sixties (Kawai, 1969). Shufford, et al., 1977, pointed both to the potential and orientation aspects of PVDF films as alternatives to standard strain gauges for monitoring composites. In relation to the calibration of PVDF sensors as alternatives to foil strain gauges Sirohi and Chopra, 2000, have considered how this aspect should be factored into the correction factors. Not to consider piezo-orthotropy can result not only in passive measurement errors but also in dynamic effects whenever the sensors are used as actuators, as shown in the study by Sokhanvar, et al., 2007. The number of investigations in the literature concerning the experimental evaluation PVDF material properties is somewhat limited, but the studies by Roh, et al., 2002 and the more recent study by Seminara, et al., 2011, would suggest that the ratios of the piezo-strain coefficients in the orthogonal plane to the poling direction can—depending on the manufacturer—be up to nearly one order of magnitude.

Schaah, et al., 2007 and Ghezzo and Nemat-Nasser, 2007 have examined the three-point bend fatigue performance of laminates fitted with embedded sensors and Caneva, et al., 2007, have studied the performance of embedded PVDF sensors as Acoustic Emission devices and Meng and Yi, 2011, have used them to study the impact performance of concrete under impact testing. The conclusions from results of these studies vary widely, primarily because the interface between the sensor and the host's matrix is a fundamental issue. However, in these studies the use of PVDF films sandwiched between silver-ink electrodes within epoxy-based laminates appears to produce good interface results. In our study we shall follow up on some of the performance aspects pointed out in these two studies, noting that we use the same type of PVDF products and comparable resin systems.

2. ESTIMATION OF PIEZOPOLYMERS SENSITIVITY

We characterize the efficiency of a piezoelectric device by monitoring the experimentally measured strain sensitivity as a function of static and dynamic strains and compare these to nominal theoretical values. Here we define Sensitivity as the average strain required to produce 1 volt over its effective surface. This quantity is reported here in μstrain/volts thus a 10 μstrain /Volt sensor is more strain sensitive than a 100 μstrain /Volt sensor. The inverse ratio defines the device as an actuator. As we shall see, piezo-polymer

sensors are sensitive dynamic strain gauges but poor actuators (especially as they have a relatively low elastic modulus).

Based on the electromechanical properties as reported in Chrysochoidis, et al., 2013 for each of the sensors, the sensitivity range can be calculated according to the equations above, assuming $Y = 2 \sim 4GPa$ and the piezoelectric stress constant was $g_{31} \approx 0.216 Vm/N$ and given that the sensors tested had a thickness of 28μm, the sensitivity for each of the PVDF devices was in the range of $Sensitivity_{PVDF} = 40 \sim 80 \mu Strain/Volt$. The second piezo-stress constant g_{32} is not explicitly provided by the manufacturer's documentation, nor was it evident from the films the alignment of the g_{31} direction in the plane of the PVDF film, which, as we shall show can have a pronounced effect on the resulting output voltages.

3. SPECIMEN PREPARATION, MATERIALS AND SENSORS

The specimens tested were fabricated at our laboratory and consisted of glass-fibre-reinforced polymer (GFRP) sandwich panels fitted with both embedded and surface-mounted piezopolymer sensors and films. The manufacture was conducted at room temperature using the vacuum-assisted resin infusion methodology; more specifically layers of 0/90 fabric cloth (205g/m²) infused with epoxy resin over a closed-cell foam core. The lamination configuration was [(0/90)₈/Core]ₛ. A low volume-fraction GFRP system was selected to visually track the transducers in the specimens and, because it is nonconductive, the ease of electrically wiring the transducers located inside the plates. The epoxy resin system and core materials used and their properties are reported in Chrysochoidis, et al., 2013.

Three different types of piezopolymer devices were used, all manufactured from poled 28μm-thick PVDF (polyvinylidene fluoride). Surface-mounted sensors with and without protective 88.5 μm thick Biaxialy Oriented Polyethylene Terephthalate (BoPET) coating was used. The active electrode surface area of the patch sensors is relatively small (30x12.19 mm²) and can, as we shall show, be used as a dynamic strain gauge. For embedding applications within the thickness of the composite laminate, i.e., between two successive composite plies, a larger film sheet of 190x130 mm² was used without protective film, ensuring direct contact between the silver-ink electrode and the layers of glass-fibre reinforcement. The electromechanical properties of the PVDFs are reported in Chrysochoidis, et al., 2013.

We manufactured two sandwich composites of dimensions (LxWxT) 280x100x34mm³. During the fabrication of the panels, the large piezopolymer film sheet was placed in between the upper-most layers of the laminate, but rather than simply laid; it was folded over along the longitudinal direction over an area of 190x65 mm². The purpose of this was motivated by two aspects:

1. The width of the film was wider than the width of the sandwich panel, and cutting the film in half whilst preserving the integrity of the electrodes was not feasible. Folding it allowed us to fit it within the specimen width and preserve the electrical functionality.

2. One aspect of our study concerns embedding sensors for energy- harvesting applications. Given that the voltage is proportional to the effective strain, folding a film would be equivalent to placing two sensors of half the width over the same strain field, which optimizes the strain energy capture field.

An extra distribution ply was inserted between the two faces of the folded sensor in order to improve the flow of the resin infusion between the folded PVDF layers. The folded sensor was placed at the penultimate layer of the composite laminate nearest the surface. The electrodes of the folded sensor are connected to fine wires that pass, through-thickness, out of the laminate and exit normal to the panel surface. For material property repeatability, both specimens were fabricated in a single resin infusion batch. Both specimens exhibited similar composite skin thickness and quality; indicating a uniform resin infusion process. However, there was a minor difference in the specimens in so far as the location of one of the large film sensors shifted by 2mm with respect to the center line. Otherwise, the sensor type and

dimensions were nominally equal. In order to monitor and, eventually calibrate the piezopolymer-based sensors, three unidirectional, 350 Ω, 10mmx30mm- strain gauges were positioned in a row along the length of the specimen surface; the first was closely located in between the two piezopolymers, and a further two at a distance of 85mm away from the mid-length. The configuration of specimen S1 with the locations of the piezopolymers as well as the strain gauges is illustrated in Figure 1.
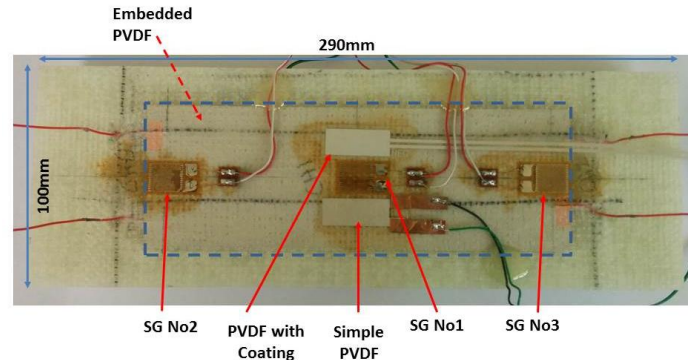

Figure 1. Foam core sandwich specimen No1 with embedded piezopolymer film sheet and attached piezopolymers and strain gauges.

4. EXPERIMENTAL METHOD

The experimental campaign consisted of cyclic testing in a three-point bending configuration. The lower, tensile face housed all the PVDF sensors and strain gauges. The general procedure consists of applying a dynamic load combined with a static offset at varying levels of amplitude. In order to monitor the effects of path sensitivity on fatigue capacity, two differing load combinations of cycle amplitude and static offset were chosen but sequenced to arrive at the same cumulative service-history demand.

4.1 Experimental Setup Measuring and control equipment

The experimental setup is illustrated in Figure 2a. A 50KN MTS testing frame was equipped with a three-point bending tool according to ASTM C393, bending testing standard specifications for composite materials (ASTM C393/C393M, 2012). The PVDF sensors and strain gauges were located on the tensile face of the three-point bending configuration, in order not to damage them as a result of the concentrated mid-span bearing loads on the compression face of the panel.

The signal conditioning and data were sampled using a National Instruments platform. For each test there was synchronous acquisition of the voltage from each PVDF sensor, the applied piston displacement, and the resultant force using an SCXI-1140 module. Simultaneously, the strains were recorded on an SCXI-1520 strain gauge conditioning module (Quarter Bridge configuration). The machine was operated in dual loop control, consisting of an outer loop in displacement control, in turn driven by an inner loop based on strain feedback, from the central strain gauge mounted at specimen mid-span. More specifically, the displacement loop was actuated by a proportional-strain-error feedback loop until the desired levels of strain (dynamic and static) were achieved. The computation of the strain-error loop signals was performed in Labview and was then used to generate a voltage signal from the analogue output of an NI-6229 board, which, in turn, drove (through the external-input source) the MTS controller.

(a)
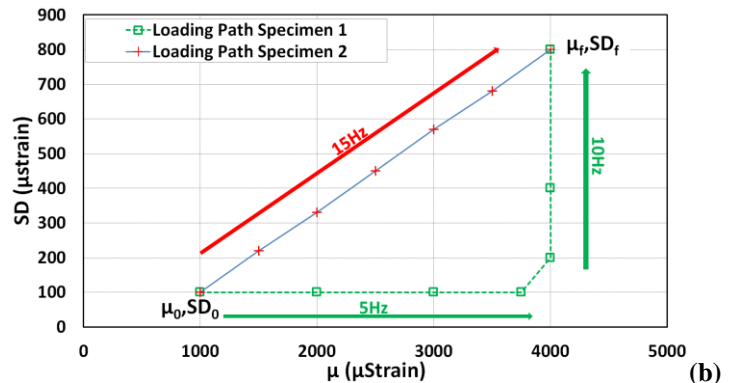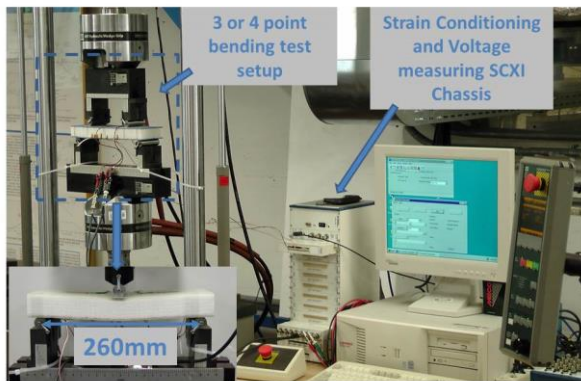
Figure 2. (a)Experimental setup for quasistatic testing; (b) The two fatigue testing loading paths applied on Specimen No1 and Specimen No2 respectively.

4.2 Dynamic range of Piezo-devices

Piezoelectric devices are also electrical capacitors; so their performance is highly frequency-dependent with no DC output. The application of a dynamic load generates a charge between the two electrodes on either side of the PVDF film which then discharges with a time-constant proportional to the capacitance and the resistive load. In effect, piezoelectric polymer sensors, when loaded with a parallel resistance, act as an electrical resonator having a -3dB cut-off frequency given by $f_c = 1/2\pi RC$, where R is the resistive load and C is the capacitance of the device. The effect of this dynamic cut-off frequency is such that at static and low frequencies well below fc, the output generated by the device will be proportional to the rate of change of strain (hence very low electromechanical transduction); whereas for excitations above fc, the output will be constant for a given strain amplitude; i.e., a dynamic self-excited strain gauge. The effective gains observed across the terminals of a PVDF sensor will depend on the impedance miss-match of the sensor, the measuring device and the frequency range of the phenomenon being measured. Because the input impedance of our measuring instrument is more than 1 GΩ we can assume an open circuit measurement on the input voltage. We shall discuss this aspect further below.

PVDF sensors are floating (non-earthed) source voltages, so in order to avoid voltage drift from leakage currents when connected to measurement instruments, a resistance is connected in parallel to the sensors terminals. The magnitude of the resistance can also be chosen to tune the cut-off frequency; typically we chose 10 MΩ or 1 MΩ in order to optimise the output voltage for our experimental campaign. The effect of the load resistance on the measured voltage (gain and phase) for each of the oscillation frequencies applied on the specimen is reported in Chrysochoidis, et al., 2013.

4.3 Fatigue Loading Paths

Each specimen's loading history was composed of seven individual static and dynamic loading steps. A static bending load was first applied up to a target mid-span strain level (as measured by gauge SG1). The second control parameter was defined by the magnitude of dynamic oscillation and is expressed as the

Standard Deviation of the strain around the mean static strain. The static and dynamic strain parameters were controlled by sampling the data and making the statistical calculations over 10 cycles. As mentioned above, different loading paths were performed for each specimen, as illustrated in Figure 2b. In one scheme we impose a constant frequency and dynamic strain $SD(\varepsilon)$ whilst increasing the static strain offset $\mu(\varepsilon)$, followed by a final large increase in the fatigue amplitude to reach $\varepsilon(\mu_f, SD_f)$. In the second mode, we gradually increase both fatigue and static amplitudes until we arrive at the same end point $\varepsilon(\mu_f, SD_f)$. Every individual point on the graph is described by the mean static strain $\mu(\varepsilon_i)$ and the standard deviation of the oscillation strain $SD(\varepsilon_i)$. The oscillation frequencies chosen were as follows: 5 Hz for Specimen S1 while the oscillation standard deviation remained constant at 100 μstrain, and 10 Hz for the remaining sets at constant mean static strain of 4000μStrain. For Specimen 2 the forcing frequency was 15Hz for the total duration of the loading path. The total number of exercise cycles was just over 6milion for both specimens.

5. RESULTS AND DISCUSSION

5.1 Preliminary experimental assessment of sensitivity

Before undertaking the extensive fatigue tests, and in order to compare to baseline data, both specimens were subjected to three parametric sensitivity analyses; the first consisted of cyclic three point bending tests of 1000-1200 cycles at frequencies in the range between 1-10 Hz in steps of 1Hz, keeping the standard deviation of the strain amplitude of SG1 at 300μstrain. The second consisted of three point bending tests with increasing standard deviation of the strain amplitude in the range 50-500μStrain with oscillation frequency at 5Hz. The third was the same as the second but with the frequency set at 10Hz.

In all parametric studies the static offsets were in the range of 1000μStrain. The full set of results for the embedded sensor is reported in Chrysochoidis, et al., 2013. The ensemble mean and standard deviations of the sensitivity measured for each of the sensors, for all the three different parametric studies mentioned are given in Tables 1 & 2. The data show that the sensitivity appears not to be greatly affected in the parametric range given above. For the small sensors, the sensitivity was calculated with respect to the strain recorded from SG1. For the larger, embedded, film sheet the sensitivity was calculated with respect to the average strain measured from all the three strain gauges across the sensor length; (we evaluated the average strain field, implying simple bending theory, from the individual strain gauges along the length as $\bar{\varepsilon} = (2\varepsilon_1 + \varepsilon_2 + \varepsilon_3)/4$).

Whereas the correlation with the predicted values, for the two small piezopolymer sensors, lies in the range of the analytically estimated values (40 to 80 μstrain/volt), the larger (folded) embedded film sheet for both specimens presents a significantly lower than expected average sensitivity, varying between 180 and 200 μstrain/volt. The discrepancy cannot be trivially explained by the fact that by folding the sensor the measured voltage is halved as, in principle, two films of half the width, when exposed to the same strain field, would measure the same voltage but would generate half the energy each (this is by virtue of having their capacitance halved, but keeping all other factors equal, the piezo-capacitance is proportional to the effective electrode area). Given that this discrepancy was repeatable, not only from one specimen to the next, but also for the full range of fatigue data, we conjectured that we had folded the film in the plane g_{32} and not g_{31}.

Table 1. Sensitivity factor and respective standard deviation of sensitivity for each of the sensors for infinite input impedance on the input terminals ([1] in g_{32} direction).

	Sensitivity (µstrain/volt)		Standard Deviation (µstrain/volt)	
Sensor	**Specimen 1**	**Specimen 2**	**Specimen 1**	**Specimen 2**
Protective film	*51.6*	*62.3*	*1.6*	*1.7*
No protective film	*47.4*	*46.6*	*1*	*0.8*
Embedded[1]	*184.9*	*190.5*	*7.7*	*9.7*

Table 2. Mean sensitivity and respective standard deviation for each of the sensors for increasing oscillation standard deviation in the range 50 to 500 µstrain when oscillation frequency was set at 5Hz and 10Hz ([1] in g_{32} direction).

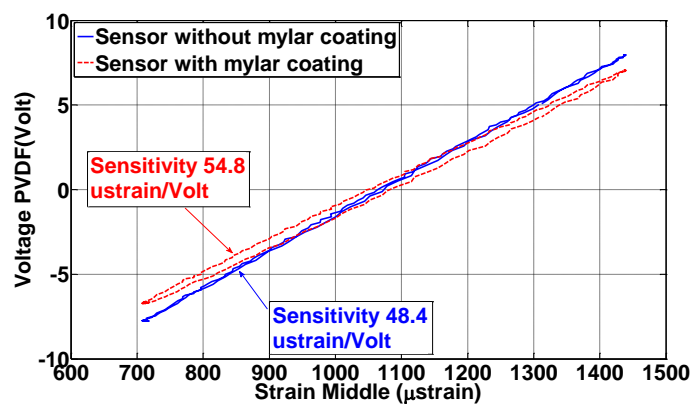|	5Hz				10Hz			
	Sensitivity (µstrain/volt)		Standard Deviation (µstrain/volt)		Sensitivity (µstrain/volt)		Standard Deviation (µstrain/volt)	
Sensor	**Specimen 1**	**Specimen 2**	**Specimen 1**	**Specimen 2**	**Specimen 1**	**Specimen 2**	**Specimen 1**	**Specimen 2**
Protective film	55.8	65.3	5.8	3.3	55.2	59.6	1.65	2.17
No protective film	52	48	8.6	1.8	46.4	46.15	1.3	0.85
Embedded[1]	184	194.5	8.1	2.9	200	188.8	12.2	10.9

Figure 3. Effect of sensor coating on the relative sensitivity measured on the two different sensors

In order to clarify the issue we manufactured another specimen, S3, similar to the other two, consisting of a simple surface-mounted PVDF sheet with CU/Ni metallized electrodes from the same manufacturer, and fitted with ready-mounted pin connectors. On the specimen we generated a constant strain over the

length of the sensor in a four point bending configuration. The results revealed that the measured sensitivity was 54 µStrain/V which falls within the expected theoretical range. We contacted the PVDF manufacturer [Personal communication with R. Brown, Measurement Specialties] who suggested a value for g_{32} in the range $[0,35]\, pC/N$. More importantly, we were informed that the principal stretching direction during poling was orthogonal to the folding axis of the embedded folded films; hence the much lower voltage obtained compared to the patch sensors. It was also confirmed to us that the g_{31} axis for the PVDF mounted on S_3 coincided with the long axis of the; hence the consistency of the strain sensitivity obtained for this configuration.

Another aspect that generates a difference in performance is the use of protective polymer coating: the presence of this coating appears to generate a pronounced hysteresis loop, normally not present in the unprotected sensor. In Figure 3 we show measurements, taken during one representative cycle, of the protected and unprotected sensors on specimen S1 when driven at 5Hz. The red hysteresis loop captures the effect of the coating, whereas the response of the bare sensor appears to be completely linear. This observation was also observed for specimen S2. The most probable reason of this hysteretic behaviour is that the 88.5 µm coating layer generates non-linear forces between the interface of the PVDF film and the composite laminate; the loss-coefficient manifests itself as a hysteresis loop in the voltage versus strain plane. This behavior clearly shows how the PVDF sensor response is sensitive enough to reveal the presence of any discrepancy in the direct load transfer. We monitored the time-lag for both specimens as a function of oscillation frequency and noted a marked correlation to the oscillation period, indicating that the phase-lag was frequency independent and constant at approximately 50 mRad. We conjecture that because this phenomenon is probably associated with shear lag through the protective coating material rather than a viscoelastic effect. This phenomenon is probably present in the bare piezo-polymers but so small that it was not discernable with the time step resolution of our data acquisition, which was set at 1kHz.

5.2 Fatigue Loading

The testing procedure was performed according to the loading history reported in Figure 2b; but we note that in both cases they merge after the first 6 million cycles (7 loading sets). The campaign consisted of individual concatenated daily-fatigue experiments of about 10 hours duration. Between each experiment, the specimen was completely unloaded. For specimen S1 the total loading history was divided into 50 daily experiments at 5 and 10Hz (5 Hz up to four million cycles and 10Hz till the specimen failure as shown in Figure 2b), but only 22 days for S2 because the loading frequency was increased to 15 Hz.

Sensor voltages may exceed input levels for electronic equipment; so in order to attenuate these voltages and eliminate the drift currents, a resistive load was placed in parallel (we used 10MΩ for specimen S1 up to the completion of 4million cycles and 1MΩ afterwards). For S2 the resistance was 10MΩ up to the completion of 6 million cycles, and only for the last loading set we decreased this to 1MΩ. For all cases the voltage attenuation correction coefficients were used in order to obtain the effective voltage outputs.

Both specimens failed in the range of 6.1 to 6.2 million cycles. For both cases, failure was initiated by local crushing of the core material immediately below the central bearing roller; followed by localized shear buckling failure of the skins. The failure was not catastrophic, but rather was noted by the fact that the specimen was unable to provide the sufficient stiffness to proceed with the control strains demanded. In other words, the central span began to drift downwards without any apparent increase in the applied load. Given this mechanism, we also conjecture that this was accompanied by a progressive shift of the neutral axis of the sandwich panel resulting from the damage to the localized crushing in the top bearing area. Further loading propagated the damage, resulting in the characteristic shear core failure.

The sensitivity of each of the three piezo-polymer sensors as a function of the number of cycles during the fatigue testing is presented in Figures 4 (a) and (b) for the embedded and the patch piezopolymers respectively. Each point in the plots represents the mean sensitivity for every individual experiment. The sensitivities of each sensor presented only slight variations during the fatigue loading history; but the performance of the embedded piezo-polymer film sheets is of particular interest as they were introduced in the composite skin at the penultimate ply in folded form, which could potentially be a weak area for delamination initiation. The general trend for both specimens is that, with increasing duty cycles, the strain required to produce one volt increases, which could be indicative of some form of degradation, either in the sensor, the laminate or the interaction between both. We conjecture that this effect results from the formation of micro-cracks at the tension face, which remain hidden and may lead to sensitivity degradation. This can potentially be considered as a local damage indicator for the sensor covered area (other sensitivity factors, e.g. temperature, being assumed constant). However, embedded sensors were shown to be capable of operating and generating voltages up to the point of incipient core crushing as seen in Figure 4 (a) accompanied by an increase to the strain/volt ratio of both specimens. The sensitivity of surface-mounted sensors is repeatable and falls within the expended range, but the scatter of the surface-coated sensors is evident in Figure 4 (b). What is also apparent is that given the extensive strain range and high duty cycles, the capacity of such sensors to operate continuously exceeds the suggestions of some authors to limit working strain levels to the order of 150μstrain (Sirohi and Chopra, 2000).

In Figures 5 (a) and (b) we present the sensitivity as a function of the dynamic strain, and we report the dynamic strain amplitude in standard deviation from the mean (i.e., the RMS amplitude minus the static mean). For the embedded film sheets, shown in Figure 5 (a), the sensitivity as a function of dynamic amplitude appears to be only marginally affected by the loading path (for S1 the 20 μstrain/volt jump corresponding to the increases in the static load shown in Figure 2b). The gradual change seems to be also captured by specimen S2 following the 2nd loading path in Figure 2b. However, in spite of the noticeable path differences both specimens performed similarly and tend to reach the same sensitivity values as they approach the merge point ε (μ_f =4000με, SD_f =800με), after which both specimens fail in approximately 100 and 200 kCycles for S1 and S2 respectively. These results seem to validate the repeatability of the specimen's performance, and indicate that the ultimate structural fatigue performance is not drastically affected by the loading history but, ultimately, by the limiting structural load.

Turning our attention to the actual voltage output, in Figures 6 (a) to (b) we show the generated voltage as a function of the number of cycles. The embedded folded film sheet can, at most, generate voltages up to 2 Volts even at the highest strains (Figure 6 (a)). The reason for this low voltage is due to two factors: a) we have established that the strain field in bending is oriented in the g_{32} coefficient direction, and b) given the three-point bending configuration the average strain field over the film length has reduced the effective average strain field and, hence, the charge generated. The voltage levels recorded for the surface-mounted sensors, Figure 6 (b), are significantly higher, but we note again that the sensitivity range of those sensors fitted with the protective coating is prone to inconsistency as seen by the greater variation in the slopes compared to the simple, untreated, sensors.
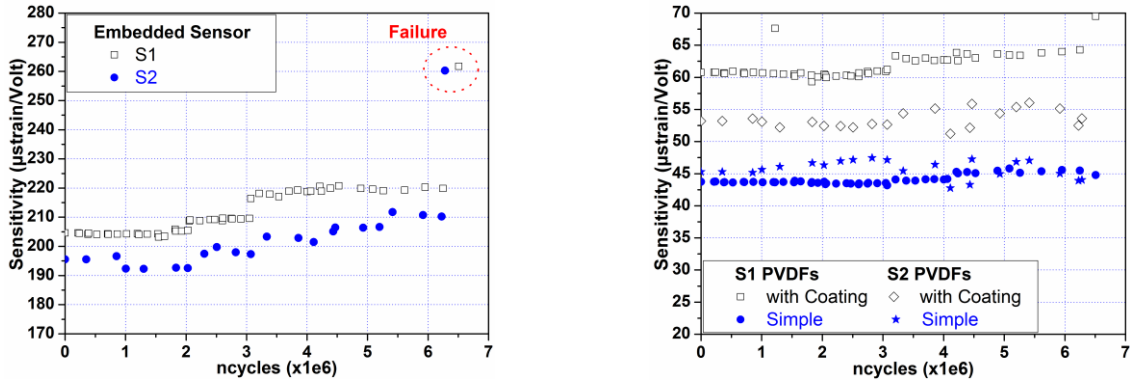
Figure4. Variation of sensitivity as a function of the number of cycles for both specimens (a) embedded piezopolymer and (b) Small surface attached PVDF sensors
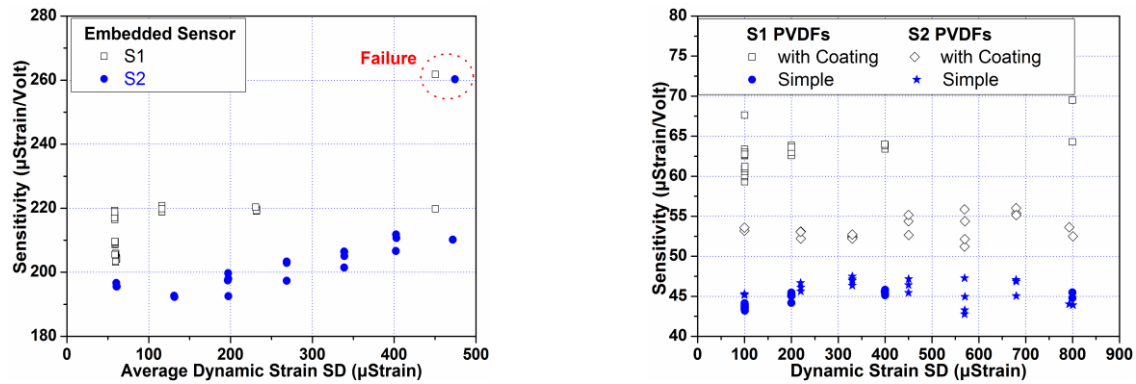

Figure 5. Variation of sensitivity as a function of the standard deviation of the dynamic applied strain for (a) embedded piezoelectric film sheet and (b) attached PVDF sensors.
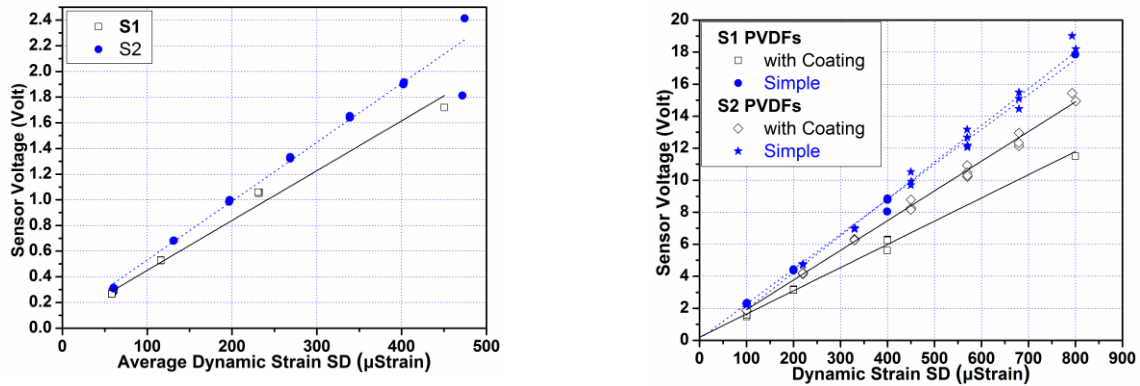

Figure 6. Sensor voltage versus the standard deviation of the dynamic applied strain for (a) Embedded sensor (b) surface attached PVDFs.

6. CONCLUSIONS

In this study we have shown that piezo-polymer sensors, either mounted onto, or embedded into, the laminates of sandwich panels, exhibit stable high strain sensitivity for a wide range of static and fatigue

strain loading. It has also been shown that it is possible to embed larger sheets of piezo-polymer within the composite laminate during the manufacturing process, providing the host structure with the added potential benefit of an in-built energy-harvesting capability.

The electromechanical sensitivity measured for surface-mounted piezopolymer sensors falls within the expected range of the theoretical values (based on the manufacturer's PVDF material data sheet). We found that the sensitivity of the larger folded embedded film sheet was also within the expected range when piezo-orthotropy is factored into the analysis.

For all sensor configurations tested, the performance appeared to be stable in the range 1-15 HZ, but the presence of even a thin layer of protection coating on the sensor results in hysteretic strain-voltage response. This hysteresis manifests itself as an-out-of-phase oscillation of the generated voltage as a function of the applied strain and it was found that the phase lag is constant in the range of frequencies studied, indicative of a rate-independent hysteretic process, possibly shear lag.

Our experimental campaign also revealed that if the sensors are well embedded or bonded onto the structure they are not significantly affected by the fatigue-loading history (i.e., differing parametric combinations of static and dynamic strain amplitudes), and they can operate in significantly high strain fields. However, the slight reduction of the sensitivity recorded as a function of the number of cycles, is possibly a consequence of the micro-crack formation on the tension-loaded face.

We should note that due to failure initiated on the compressive and not the tensile side of the sandwich, both the surface-mounted and embedded sensors were still active even after catastrophic failure of the panel. This performance would imply that the intralaminar bonding surface of the large embedded piezopolymer film sheet was sufficiently sturdy to ensure consistent shear transfer from the laminate to the sensor at high loading strains.

PVDF devices can potentially provide the requested voltage at low working strain levels for supplying an energy harvesting circuit at voltage levels of 3-6 volts, which are satisfactory for commercially-available electronic energy harvesting rectification circuits. However, given the biased piezoelectric coefficients, and the rather low energy-transduction efficiency, the orientation of the films should be clearly identified in order to align the film along the optimal direction.

PVDF sensors have some drawbacks compared to piezo-ceramics, particularly as regards the stability and sensitivity at higher temperatures. On the other hand, their low modulus, thinness, high-strain-to-failure and lower cost offer some advantages when applied in conjunction with flexible structures and composite materials. The orthotropy of some PVDF films can also be exploited further by ensuring that the piezo-electric coefficient normal to the measuring direction is minimized, thus reducing the complexity of calibrating the sensor for Poisson and direct coupling effects. In this sense, PVDF films offer an advantage over piezoceramics which, due to their homogeneous piezo-properties, may require both Poisson and shear-lag correction. Finally, the high signal-to-noise ratio can be easily exploited by adapting PVDF sensors to low cost energy-harvesting and data acquisition sensors, once due care has been made for appropriate impedance matching.

We conclude that for low-cost applications where multiple (hundreds) of sensors are required for field monitoring, PVDF-based sensors, especially embedded systems, may provide a satisfactory solution for dynamic strain monitoring and structural diagnostic without the requirement of additional power supply.

REFERENCES

ASTM C393/C393M, 2012. *Standard Test Method for Core Shear Properties of Sandwich Constructions by Beam Flexure.*

Bronowicki A, McIntyre L, Betros R and Dvorsky G 1996 Mechanical validation of smart structures. *Smart Mater. Struct.* **5** 129-139

Caneva C, De Rosa I M and Sarasini F 2007 Acoustic Emission Monitoring of Flexurally Loaded Aramid/Epoxy Composites by Embedded PVDF Sensors *J. of AE* **25** 80-91

Chow W T and Graves M J 1992 Stress analysis of a rectangular implant in laminated composites using 2-D and 3-D finite elements *Proc. AIAA/AHS/ASME/ASCE/ASC 33rd Structures,Structural Dynamics and Materials Conference* (Dallas TX) 848–861

Chrysochoidis N A, Mainetti S, Ruotolo E and Gutierrez E 2013 Objective 2:Conduct Experimental Activities on Performance of Sensor- Equipped Composite Elements (Ispra IT) *Publications Office of the European Union*

Crawley E F and De Luis J 1987 Use of piezoelectric actuators as elements of intelligent structures *AIAA J.* **25** 1373–1385

De Rosa I M and Sarasini F 2010 Use of PVDF as acoustic emission sensor for in situ monitoring of mechanical behaviour of glass/epoxy laminates *Polym. Test.* **29** 749–758

Elvin N, Elvin A and Choi D H 2003 A self-Powered Damage Detection Sensor *J. Strain Anal. Eng. Des.* **38**(2) 115-124

Elvin N G, Elvin A A and Spector M 2001 A self-powered mechanical strain energy sensor *Smart Mater. Struct.* **10** 293-299

Ghezzo F and Nemat-Nasser S 2007 Effects of embedded SHM sensors on the structural integrity of glass fiber/epoxy laminates under in-plane loads *Sensor Systems and Networks: Phenomena, Technology, and Applications for NDE and Health Monitoring SPIE* **6530**

Hansen J and Vizzini A 2000 Fatigue Response of a Host Structure with Interlaced Embedded Devices *J. of Intell. Mater. Syst. and Struct.* **11** 902-909

Kawai H 1969 The Piezoelectricity of Polyvinylidene Fruoride *Jpn. J. Appl. Phys.* **8** 975

Mall S and Coleman J 1998 Monotonic and fatigue loading behavior of quasisotropic graphite/epoxy laminate embedded with piezoelectric sensor *Smart Mater. Struct.* 7 822-832

Meng Y and Yi W 2011 Application of a PVDF-based stress gauge in determining dynamic stress-strain curves of concrete under impact testing *Smart Mater. Struct* **20** 065004

Roh Y, Varadan V V and Varadan V K 2002 Characterization of All the Elastic, Dielectric, and Piezoelectric Constants of Uniaxially Oriented Poled PVDF Films *IEEE Trans. Ultrason., Ferroelectr., Freq. Control* **49**(6) 836-847

Schaah K, Rye P and Nemat-Nasser S 2007 Optimization of Sensor Introduction into Laminated Composites *Proceedings of the 2007 SEM Annual Conference and Exposition on Experimental and Applied Mechanics* (Massachusetts)

Seminara L, Capurro M, Cirillo P, Cannata G and Valle M 2011 Electromechanical Characterization of Piezoelectric PVDF Polymer Films for Tactile Sensors in Robotic Applications *Sensor Actuat. A-Phys.***169** 49-58

Shufford R, Wilde A, Ricca J and Thomas G 1977 Piezoelectric Polymer Films for Application in Monitoring Devices *Massachusetts: Army Materials and Mechanics Research Center*

Shukla D and Vizzini A 1996 Interlacing for improved performance of laminates with embedded devices *Smart Mater. Struct* **5** 225-229

Sirohi J and Chopra I 2000 Fundamental understanding of piezoelectric strain sensor *J. of Intell. Mater. Syst. and Struct.* **11** 246-257

Sokhanvar S, Zabihollah A and Sedaghati R 2007 Investigating the effect of the orthotropic property of piezoelectric PVDF *Trans. Of CSME* **31**(1) 111-125

Tang 'RAY' H-Y, Winkelmann C, Lestari W and Saponara V 2011 Composite Structural Health Monitoring Through Use of Embedded PZT Sensors *J. of Intell. Mater. Syst. and Struct.* **22** 739-755

Warkentin J and Crawley F 1991 Embedded electronics for intelligent structures *32nd Strucrures , Structural Dynamics and Materials Conference* (Baltimore) 1322–31

Yocum M, Abramovich H, Grunwald S and Mall A 2003 Fully reversed electromechanical fatigue behavior of composite laminate with embedded piezoelectric actuator/sensor. *Smart Mater. Struct* **12**(4) 556-564